Biointerface Research in Applied Chemistry
Open-Access Journal (ISSN: 2069-5837)

Article
Volume 13, Issue 2, 2023, 190
https://doi.org/10.33263/BRIAC132.190

Biofabrication of Zirconia Nanoparticles: Synthesis, Spectral Characterization and Biological Activity Evaluation against Pathogenic Bacteria

Nagaraj Muthulakshmi [1], Arumugam Kathirvel [2], Ramasamy Subramanian [3], M. Senthil [1,*]

[1] Department of Chemistry, Kandaswami Kandar's College, Velur 638182, Tamil Nadu, India; muthilakshmi.nagaraj@gmail.com (N.M.); senthilmk1975@gmail.com (M.S.);
[2] Department of Chemistry, K.S. Rangasamy College of Arts and Science, Trichengode 637215, Tamil Nadu, India; chemkathirvel@gmail.com (A.K.);
[3] Department of Chemistry, Sun Arts and Science College, Tiruvannamalai 606755, Tamil Nadu, India; ksrcasssubu@gmail.com (R.S.);
* Correspondence: senthilmk1975@gmail.com;

Received: 3.01.2022; Accepted: 5.02.2022; Published: 3.04.2022

Abstract: The eco-friendly fabrication of zirconia nanoparticles (ZrO_2 NPs) using *Guettarda speciosa* (*G. speciosa)* leaves extract was achieved. Three samples were prepared by using different concentrations of the precursor solution. The synthesized samples were characterized by Ultraviolet-visible spectrophotometer (UV–Vis), Fourier transform infrared spectrometer (FTIR), X-ray diffraction (XRD), Scanning electron microscope (SEM), Energy-Dispersive study (EDS), High-resolution transmission electron microscope (HR-TEM) coupled with selected area diffraction pattern (SAED). The ZrO_2 NPs were in a tetragonal crystal structure, which was established by using XRD pattern and the average crystallite size was in the range of 6-9 nm. The ZrO_2 NPs were in spherical morphology, and no agglomeration was confirmed by FESEM and HR-TEM analysis. Antibacterial activity ZrO_2 NPs was tested against oral bacteria, *Escherichia coli, Bacillus substilis*, *Salmonella typhi*, and *Pseudomonas aeruginosa*. The results revealed that the green synthesized ZrO_2 NPs nanoparticles are potential antibacterial properties. From the results and discussion, leaves extract of *G. speciosa* is a potential natural reducing agent, and hence, ZrO_2 NPs could be used for dental application.

Keywords: green fabrication; zirconia nanoparticles; *Guettarda speciosa;* antibacterial activity.

© 2022 by the authors. This article is an open-access article distributed under the terms and conditions of the Creative Commons Attribution (CC BY) license (https://creativecommons.org/licenses/by/4.0/).

1. Introduction

Nanoparticles (NPs) of less than 100 nm are widely used in nanoscience [1]. Nan bioscience is an emerging field with tremendous applications such as biological science and pharmaceutical technology. Recently, metal oxide nanoparticles have been focused on due to their remarkable properties and applications. In particular, the fabrication of nanoparticles has attracted much attention in nanotechnology research, as there is increasing demand in industries and medical sectors such as fillers, disinfectants, optics, antimicrobial agents, drug delivery, and catalytic products [2]. Metal oxide nanoparticles such as ZnO, CuO, CeO_2, and ZrO_2 NPs have been studied for their biological and biomedical applications [3,4]. Zirconium oxide (ZrO_2), also known as zirconia, is a versatile material that has been widely used as a photocatalyst [5,6]. It has enhanced thermal, mechanical, catalytic, and corrosion properties [7,8]. Various methods of synthesizing zirconia nanoparticles have been investigated for various applications [9,10]. Several methods such as precipitation, solvothermal, spray drying

system, sonochemical, hydrothermal, and sol-gel methods [11] are engaged to synthesize nanoparticles in chemical methods. However, the conventional methods required some toxic solvents, which dispose harmful residues to human health and the environment.

Thus, green synthesis is a promising way of producing various metal and metal oxide nanoparticles [12-15]. Green synthesis is a non-toxic, biodegradable, and low-cost chemical compared with the chemical synthesis of nanoparticles [16,17]. Plant extracts are very promising due to their complex chemical composition and the facilities for their extraction. They act in the synthesis as a reducer and as a capping agent preventing the agglomeration of nanoparticles during the nucleation. However, some studies use green synthesis to prepare zirconia nanoparticles [18-20]. Many other contributions are still needed due to the great genetic variability of plant species that can lead to varying chemical compositions depending upon the plant studied. This factor can interfere directly with the properties of the material obtained. Because of that, the use of different species must still be evaluated [21].

Various plant extracts have been used as a green stabilizing agent in the synthesis of ZrO_2 NPs. *Fusarium oxyporam* fungus [22], Helianthus annuus seed [23], *Rosemary* [24], *Alovera* [25], *Nyctanthes* plant [26], *Curcuma longa* tuber extract [27], *Lemon juice* [28], *Eucalyptus globuler* [29], *Lagerstro emia speciosa* [30] seaweed *sargassum wightii* [31], *Euclea nataleni*ss extract [32] and *Wrightia tinctoria* leaf extract [11], *Daphne alpine* leaves extract [33] and *Curcuma longa* extract [34] have been used as green stabilizing agents to produce ZrO_2 NPs. Green synthesis is easy and cost-effective compared with chemical methods. Also, it reduces toxic substances, which affect human health and the environment. Hence, there is a great demand for developing a safe, simple, and eco-friendly synthesizing method for nanoparticles. The phytochemicals such as carbohydrate, saponin, amino acid, flavonoid, terpenoid, and protein present in the plant extract play a key role in synthesizing nanoparticles [21,35].

There is no literature on the green synthesis of zirconia nanoparticles using *G. speciosa* leaves extract and its evaluation of the biological activity. *G. speciosa* belongs to the Apocynaceae family. It is used for treating infection, cough, cold, sore throat, dysentery, wounds, and headache as a traditional folk medicine [36]. These traditional folkloric claim the anti-inflammatory activity in murine macrophages of the methanolic extract from Indonesia [37,38].

The present work aims to synthesize ZrO_2 NPs using a simple and eco-friendly method using leaves extract of *G. speciosa* and study their effect on the morphology, followed by the examination of antibacterial activity.

2. Materials and Methods

2.1. Materials.

All the reagents used in this work, including zirconyloxychloride were analytical grade (99.9%). All the bacterial cultures such as *Escherichia coli, Bacillus subtilis, Salmonella typhi*, and *Pseudomonas aeruginosa* were purchased from a microbial culture collection, Institute of Microbial Technology, Chandigarh, India. All the reagents used were of analytical grade with the highest purity. All the solutions were prepared using distilled water.

2.2. Preparation of extract.

G. speciosa leaves were collected from Velur, Namakkal District, Tamil Nadu, India. Fresh leaves were taken from the plant and washed thoroughly with distilled water. Then, the leaves were dried under shade for a week (a better method to maintain the phytochemicals active in the leaves) before being ground into a fine powder. Then, 100 g of leaf powder was added to 250 mL of distilled water and boiled at 85°C for 2 h. The extract was cooled to room temperature and then filtered by using a Whatman filter paper and stored in a refrigerator for further use.

2.3. Synthesis of ZrO_2 NPs.

For the green synthesis of ZrO_2 NPs, different concentrations (0.02 M, 0.05 M, and 0.08 M) of precursor solution were prepared using *G. speciosa* leaves extract. The reaction mixture was heated on a hot plate with a magnetic stirrer at 85°C. The off-white precipitate was formed without adding any chemical reducing agent. The precipitate was thoroughly washed with distilled water several times. Then, the precipitate was carefully collected and dried at 100°C for 3 h. The precipitate was calcinated at 500°C for 2 h to decompose zirconium hydroxide into their oxide. Finally, the obtained nanoparticles were stored in an airtight container for further studies.

2.4. Characterization methods.

The green synthesized ZrO_2 NPs were analyzed by UV-Visible spectrophotometer (UV-1800 Shimadzu) with a resolution of 1 nm, in 200-800 nm. Functional group analysis was studied by Fourier transform infrared spectrophotometer in the frequency range of 400-4000 cm^{-1}. The crystalline phase of the samples was analyzed by the X-ray diffractometer (XRD) operating at a current of 40 mA and voltage of 45 kV with Cu-Kα radiation in the scanning range of 2θ from 10° to 80°. The formation of the particles and elemental composition of the samples were studied by SEM with the resolution 15 nm (JEOL Model JSM – 6390LV SEM) coupled with EDAX. The morphology and structure were examined using HR-TEM using Jeol/JEM 2100, operating at an accelerating voltage of 200 kV. The selected area electron diffraction (SAED) pattern was also recorded from the HR-TEM image to obtain the morphology of the nanoparticles.

2.5. Antibacterial activity.

The antibacterial activity of ZrO_2 NPs synthesized using *G. speciosa* leaves extract was studied by the disc diffusion method [39]. The green synthesized ZrO_2 NPs were examined for their antibacterial activity against clinically isolated bacterial cultures such as *Escherichia coli* (*E. coli*), *Bacillus substilis (B. substilis)*, *Salmonella typhi (S. typhi)*, and *Pseudomonas aeruginosa (P. aeruginosa)* and *Proteus vulgaris* (*P. vulgaris*). The antibacterial activity of nanoparticles was examined by the well diffusion method. Nutrient agar medium, 20 mL, was poured into the Petri-plates of 5 mm wells, and made sterile using a cork borer. Different concentrations of ZrO_2 NPs (25, 50, 75,100 μg), and 50 μL were loaded onto the wells. Ciprofloxacin was taken as a standard antimicrobial agent (25 μg). The plates were incubated at 37°C for 24 h. The diameters of inhibition zones were measured in millimeters (mm).

3. Results and Discussion

3.1. UV-Vis study.

The UV-Visible spectra of ZrO_2 NPs are shown in Figure 1 (A-C). From the figure, biosynthesized ZrO_2 NPs showed strong absorption at 224, 225, and 226 nm. It is seen that the absorption of nanoparticles is nearly the same for all the samples. Bandgap energy of A, B, and C were calculated by using the Tauc formula.

$$(\alpha h\nu)n = A(h\nu - Eg).$$

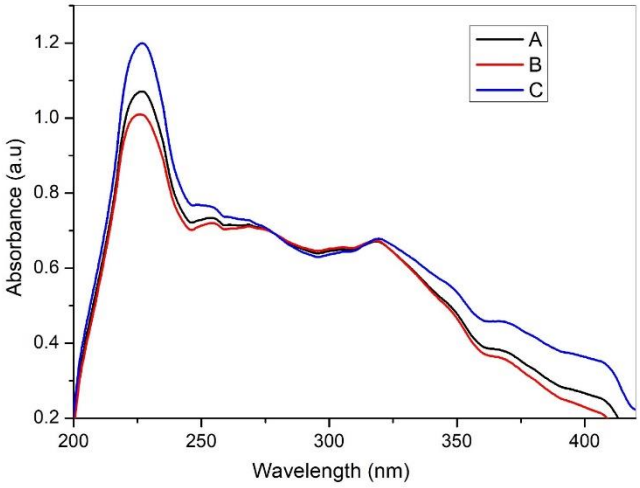


Figure 1. UV-Vis spectrum of ZrO_2 NPs; A-C represents NPs synthesized using 0.02, 0.05, and 0.08 M solution using *G. speciosa* leaves extract.

Here, α is the absorption coefficient, hν is the photon's energy, and Eg is the bandgap energy [40]. The variation of $(\alpha h\nu)^2$ versus hν is linear at the absorption edge, confirming that the nanoparticles are semiconductors with direct bandgap energy. The estimated direct bandgap energy of A sample is found to be 5.54 eV, and that for B and C is found to be 5.51 eV and 5.49 eV, respectively. The probable mechanism of phytochemicals present in the leaves extracts the reduction of Zr^{2+} to zero-valent Zr. Also the phytochemicals in leaves extract act as stabilizing as well as a capping agent in the formation of ZrO_2 NPs. This is similar to the earlier studies found in the literature that confirm the presence of ZrO_2 NPs [41]. The result denotes the extra contribution from external states for absorption in the region. The ZrO_2 NPs may have greater surface defects due to their great surface area [28].

3.2. FTIR study.

FTIR analysis was carried out to assess the possible bonds in the ZrO_2 NPs. Figure 2 (A-C) illustrates the FTIR spectra of ZrO_2 NPs synthesized using *G. speciosa* leaves extract. The ZrO_2 NPs show broad, sharp, and weak absorption bands at 3416-3132, 2323, 1621, 1402, 1047, 961, 827, 649, and 465 cm^{-1}. A broadband noticed in the range between 3416-3132 cm^{-1} reveals the presence of moisture content during sample preparation [42]. The absorption band obtained between 649-465 cm^{-1} is characteristic of Zr–O–Zr vibrations. The region between 1402-827 cm^{-1} indicates the presence of a Zr-O bond supported by the tetragonal form of ZrO_2 NPs [25].

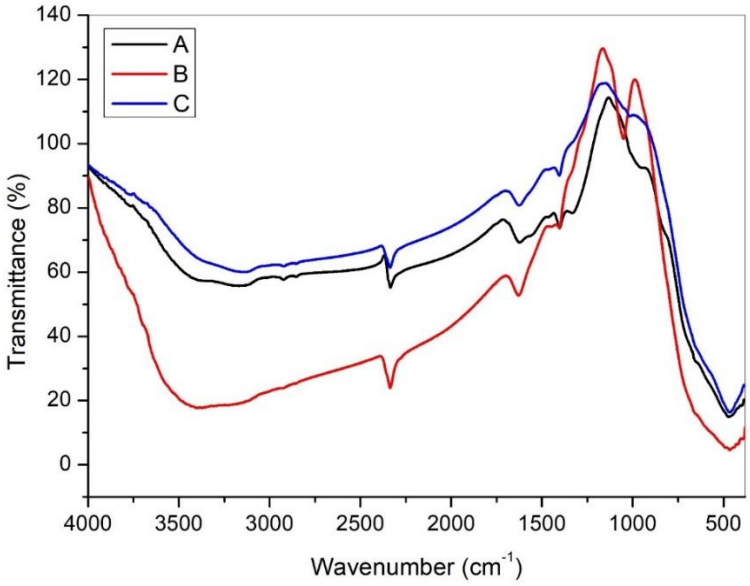


Figure 2. FTIR spectra of ZrO_2 NPs synthesized using *G. speciosa* leaves extract from (A) 0.02 M, (B) 0.05 M, and (C) 0.08 M solution.

3.3. XRD analysis.

The crystalline phase structure of the green synthesized ZrO_2 NPs was confirmed by the XRD pattern as depicted in Figure 3 (A-C). The diffraction peaks are found at 2θ = 27.55, 31.08, 35.85, 45.55, 50.85, 54.20, 60.37, 63.55 and 75.19° corresponding to the (101), (110), (112), (103), (211), (202), (220), (213) and (310) lattice planes, respectively. (JCPDS Card No: 42-1164 and 37-1484). This reveals that the green synthesized ZrO_2 NPs are in both monoclinic and tetragonal phases, found similar results from the previous report [43]. It can be noticed from the figure that the (101) plane has high intensity of showing crystals with the plane (101). The crystallite size of the particles was calculated by applying Debye-Scherrer's equation (1).

$$D = \frac{K\lambda}{\beta \cos\theta} \qquad (1)$$

Where, D is the size of the particle, λ the wavelength (0.1542 nm) with Cu-Kα radiation), β the full width at half maximum, and θ the Bragg angle. Small peaks at 27.55 show phase transition from tetragonal to monoclinic phase.

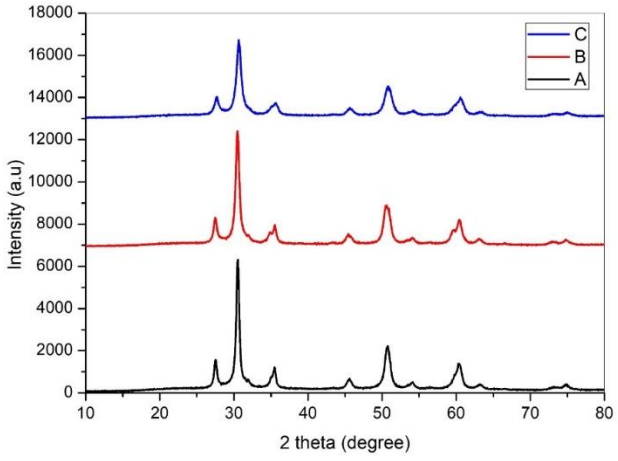


Figure 3. XRD spectra of ZrO_2 NPs synthesized using *G. speciosa* leaves extract from (A) 0.02, (B) 0.05, and (C) 0.08 M solution.

The XRD pattern of samples shows that the tetragonal-monoclinic diversified phase is formed. The peaks witnessed at 27.55 and 31.08° correspond to the (−111) and (111) planes of the monoclinic phase. The intensity of diffraction peaks corresponds to the tetragonal phase and monoclinic phase. The average crystallite of A, B, and C are found to be 6.54, 6.53, and 9.15 nm, respectively. The sharp peaks exhibited in XRD pattern reveal that the *G. speciosa* leaves extract stabilized ZrO_2 NPs is pure and crystalline.

3.4. SEM analysis.

The morphology, shape, and formation of ZrO_2 NPs were analyzed by scanning electron microscope. The SEM morphographs of the particles under two different magnifications and images are displayed in Figure 4 (A-C). The images show that the particles are irregular, quasi-spherical particles and agglomerated. The irregular shape and agglomerated particles were noticed in A, B, and C. However, the SEM images of ZrO_2 NPs prepared using 0.02M solution show that the particles are spherical and homogeneously distributed without agglomeration.

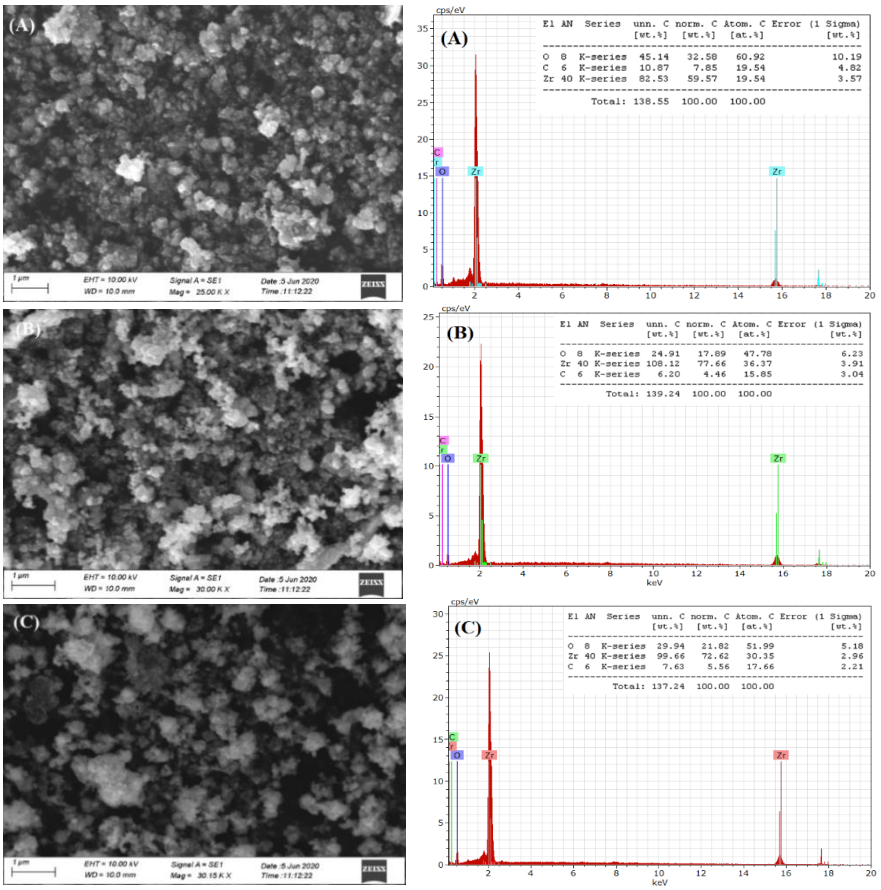


Figure 4. SEM images and EDAX spectra of ZrO_2 NPs synthesized from (A) 0.02, (B) 0.05, and (C) 0.08 M solution using *G. speciosa* leaves extract.

The chemical composition of the ZrO_2 NPs was analyzed using EDX, as shown in Figure 4 (A-C). These results exhibited peaks for oxygen and zirconium. In addition, carbon is also present in all three samples at 2-3 %. This residual carbon may be due to biomolecules present in the extract. The percentage of elemental composition is included in each EDAX spectrum.

3.5. TEM morphology study.

The shape, morphology, and lattice interplane distance of the ZrO_2 NPs were analyzed using HR-TEM with SAED pattern. HR-TEM images of A, B, and C prepared using 0.02, 0.05, and 0.08 M solution are shown in Figure 5 (A-C). The TEM images display quasi-spherical shape, and some show slight agglomerations. The high magnification micrograph was displayed in Figure 6C.

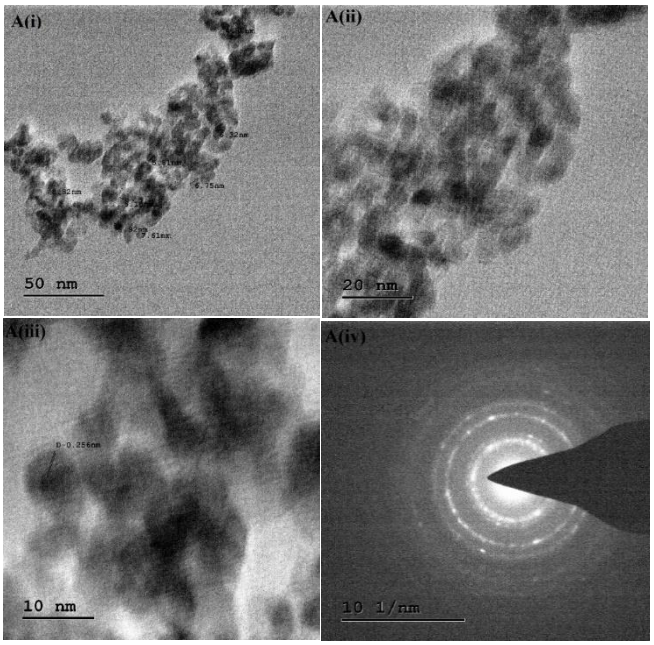


Figure 5(A). TEM images of ZrO_2 NPs synthesized from (A) 0.02 M solution using *G. speciosa* leaves extract.

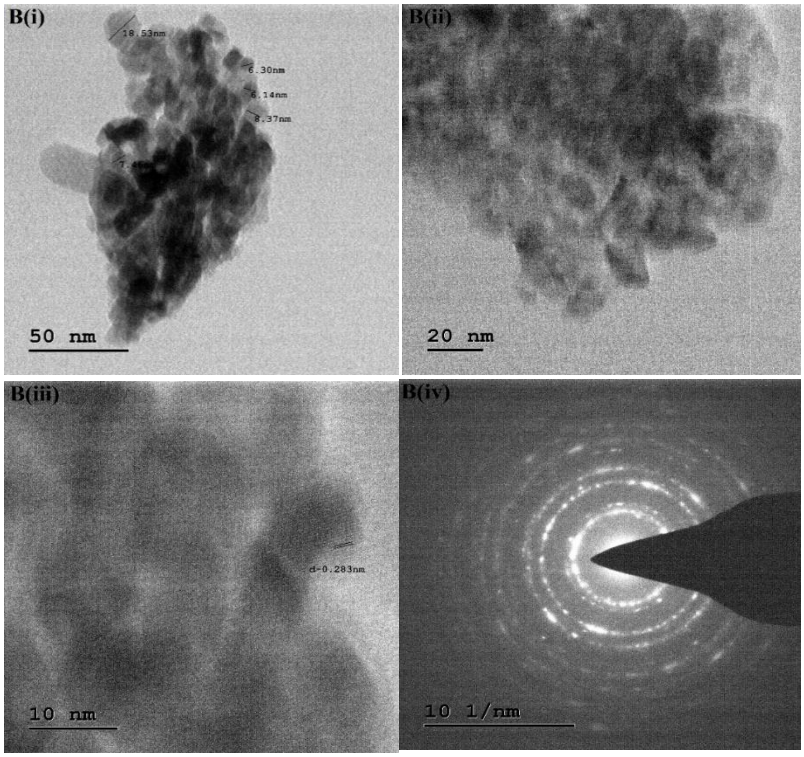


Figure 5(B). TEM images of ZrO_2 NPs synthesized from (B) 0.05 M solution using *G. speciosa* leaves extract.

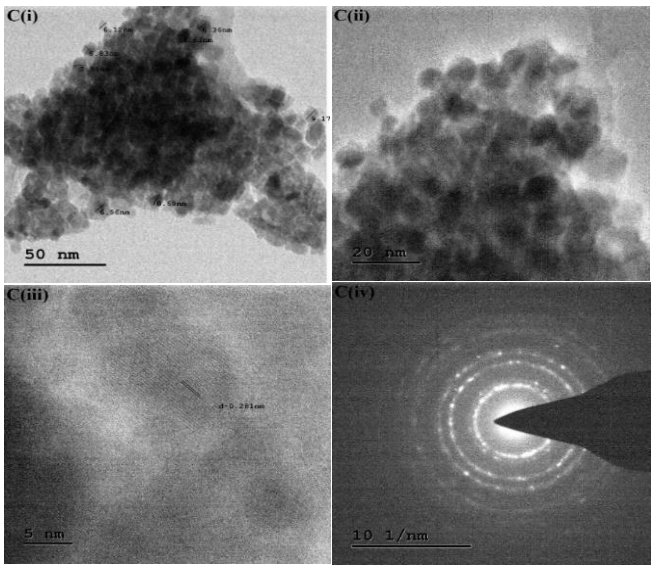


Figure 5(C). TEM images of ZrO_2 NPs synthesized from (B) 0.05 M solution using *G. speciosa* leaves extract.

The SAED image ZrO_2 NPs exhibit ring structures and slight crystalline spots as denoted in Figure 6 (A-C (iii)). These images can clearly depict lattice fringes pattern of A, B, and C at 0.256, 0.283, and 0.281 nm corresponding to the crystalline (101) plane of tetragonal ZrO_2 NPs. The clear lattice fringe observed in the TEM images further confirms the crystallinity of the samples. The lattice spacing, 0.2702 nm from the TEM image, corresponds (101) plane of tetragonal ZrO_2 NPs.

3.6. Antibacterial activity.

The antibacterial efficiency of ZrO_2 NPs was examined against *Escherichia coli (E. coli)*, *Bacillus substilis (B. subtilis*) and *Salmonella typhi (S. typhi)*, *Proteus vulgaris* (*P. vulgaris*), and *Pseudomonas aeruginosa (P. aeruginosa)* and the zone of inhibition was measured by using disc diffusion method (Figure 6).

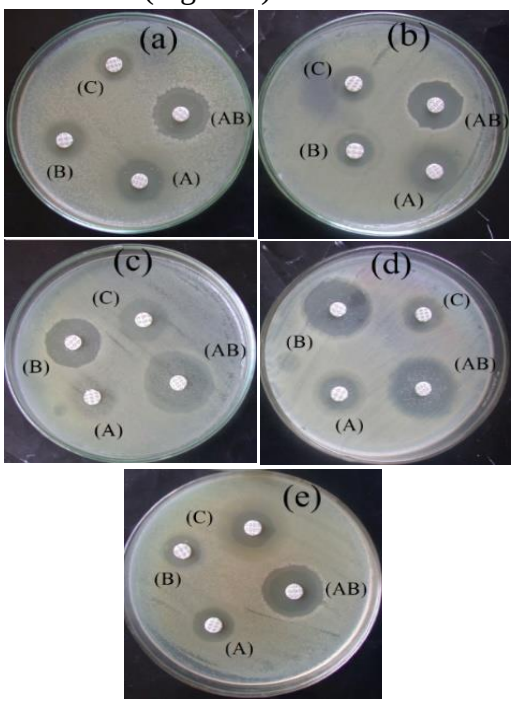


Figure 6. Zone of inhibition shown by (a) *Escherichia coli, (b) Bacillus substilis, (c) Salmonella typhi,* (d) *Pseudomonas aeruginosa* and (e) *Proteus vulgaris*. Each plate (AB) Ciprofloxacin antibiotic (25 µg), A, B, and C represent ZrO_2 NPs synthesized using *G. speciosa* leaves extract from 0.02, 0.05, and 0.08 M solution.

The zone of inhibition of A, B, and C were tested at the concentration of 100 µg/ml for all the bacteria. At the same time, 25 µg/ml of antibiotic was used as standard. The zone of inhibition against *E. coli* observed for A, B, and C was 10, 5, and 5 mm.

The zone of inhibition against *B. subtilis* observed for A, B, and C was 10, 8, and 8 mm. The zone of inhibition against *S. typhi* observed for A, B, and C was 15, 12, and 12 mm. The zone of inhibition against *P. vulgaris* observed for A, B. C was 5, 15, and 8 mm. Similarly, the zone of inhibition against P. aeruginosa observed for A, B. C was 8, 5, and 8 mm. 5, 15 and 8 mm. Antibiotic exhibit the zone of inhibition from 17 mm to 20 mm for all the tested bacteria. However, the bactericidal killing potential of ZrO_2 NPs is not comparable with antibiotics. The results established that ZrO_2 NPs synthesized using *G. speciosa* leaves extract to possess better antibacterial activity against all the bacterial strains. From this test, it can be considered that the ZrO_2 NPs are effective in inhibiting bacterial growth. This may be due to the interaction between bacteria and ZrO_2 NPs. Different mechanisms have been proposed for antibacterial activity. It is thought that smaller particles penetrate the cell wall, damaging the microorganism. There is an electrostatic interaction between bacteria and charged particles, which rupture the cell wall causing cell death. *G. speciosa* leaves extract stabilized ZrO_2 NPs are found to be smaller in size according to the XRD analysis, which has a large surface area that may improve the killing efficiency of nanoparticles [44].

4. Conclusions

It is established that the tetragonal spherical ZrO_2 NPs can be synthesized by *G. speciosa* leaves extract as a stabilizing agent as well as a reducing agent. The ZrO_2 NPs have obtained from 0.02, 0.05, and 0.08 M solution without adding any chemical reducing agent. The growth of spherical ZrO_2 NPs was established by UV-Vis, FTIR, XRD, SEM-EDAX, and TEM-SAED techniques. The synthesis incorporating this *G. speciosa* leaves extract led to the formation of spherical particles with sizes ranging between 4 to 9 nm. The synthesized ZrO_2 NPs exhibited a zone of inhibition against tested bacteria, showing their bactericidal efficiency. Bandgap energy calculated from the UV-Vis study gave added evidence for the formation of ZrO_2 NPs. The water-soluble biomolecules present in the *G. speciosa* leaves extract might be responsible for the formation of spherical particles. Thus, *G. speciosa* proved to be a suitable biomaterial for synthesizing ZrO_2 NPs.

Funding

This research received no external funding.

Acknowledgments

Authors thank St Joseph College, Trichy, for providing characterization facilities.

Conflicts of Interest

The authors declare no conflict of interest.

References

1. Chinnadurai, G.; Subramanian, R.; Selvi, P. Fish mucus stabilized iron oxide nanoparticles: fabrication, DNA damage and bactericidal activity. *Inorganic and Nano-Metal Chemistry* **2021,** *51*, 1-10, https://doi.org/10.1080/24701556.2020.1799401.

2. Muthuvel, A.; Jothibas, M.; Manoharan, C. Synthesis of copper oxide nanoparticles by chemical and biogenic methods: photocatalytic degradation and in vitro antioxidant activity. *Nanotechnology for Environmental Engineering* **2020**, *5*, https://doi.org/10.1007/s4120-020-00078-w.
3. Chinnadurai, G.; Subramanian, R.; Ahamed, M. Fish mucus mediated biosynthesis of copper oxide nanoparticles: spectral characterization, morphology and biological activity. *Materials Research Express* **2020**, *7*, https://doi.org/10.1088/2053-1591/abcee7.
4. Jeba, R.; Radhika, S.; Padma, C.M.; Ascar Davix, X. Antimicrobial and photocatalytic activities of Strontium Doped Zirconium Oxide nanoparticles. *Materials Letters* **2021**, *331*, https://doi.org/10.1016/j.matlet.2021.131559.
5. Rajesh, G.; Akilandeswari, S.; Govindarajan, D.; Thirumalai, K. Enhancement of photocatalytic activity of ZrO_2 nanoparticles by doping with Mg for UV light photocatalytic degradation of methyl violet and methyl blue dyes. *Journal of Material Science: Materials in Electronics* **2020**, *31*, 4058–4072, https://doi.org/10.1007/s10854-020-02953-3.
6. Felipe Vianada Silva, A.; PaulaFagundes, A.; Pier Macuvele, D.L.; Uranode Carvalho, E.F.; Durazzo, M.; Padoin, N.; Soares, C.; Riell, H.G. Green synthesis of zirconia nanoparticles based on *Euclea natalensis* plant extract: Optimization of reaction conditions and evaluation of adsorptive properties. *Colloids and Surfaces A: Physicochemical and Engineering Aspects* **2021**, *583*, https://doi.org/10.1016/j.colsurfa.2019.123915.
7. Rao, T.N.; Hussain, I.; Lee, J.E.; Kumar, A.; Koo, B.H. Enhanced Thermal Properties of Zirconia Nanoparticles and Chitosan-Based Intumescent Flame Retardant Coatings. *Applied Sciences* **2019**, *9*, https://doi.org/10.3390/app9173464.
8. Ruíz-Santoyo, V.; Marañon-Ruiz, V.F.; Romero-Toledo, R.; González Vargas, O.A.; Pérez-Larios, A. Photocatalytic Degradation of Rhodamine B and Methylene Orange Using TiO_2-ZrO_2 as Nanocomposite. *Catalysts* **2021**, *11*, https://doi.org/10.3390/catal11091035.
9. Ahmad, T.; Shahazad, T.M.; Phul, R. Hydrothermal Synthesis, Characterization and Dielectric Properties of Zirconia Nanoparticles. *Material Science & Engineering International Journal* **2017**, *1*, 4–8, https://doi.org/10.15406/mseij.2017.01.00017.
10. Zinatloo-ajabshir, S.; Salavati-Niasari, M. Facile route to synthesize zirconium dioxide (ZrO_2) nanostructures : Structural, optical and photocatalytic studies. *Journal of Molecular Liquids* **2016**, *216*, 545–551, https://doi.org/10.1016/j.molliq.2016.01.062.
11. Nabil Al-Zaqri, A.; Muthuvel, M.; Jothibas, Alsalme, A.; Fahad, A.; Alharthi, V.; Mohana, V. Biosynthesis of zirconium oxide nanoparticles using *Wrightia tinctoria* leaf extract: Characterization, photocatalytic degradation and antibacterial activities. *Inorganic Chemistry Communications* **2021**, *127*, https://doi.org/10.1016/j.inoche.2021.108507.
12. Mohamed El Shafey, A. Green synthesis of metal and metal oxide nanoparticles from plant leaf extracts and their applications: A review. *Green Processing and Synthsis* **2020**, *9*, 304-339, https://doi.org/10.1515/gps-2020-0031.
13. Zhang, D.; Ma, X.–L.; Gu, Y.; Huang, H.; Zhang, G.–W. Green Synthesis of Metallic Nanoparticles and Their Potential Applications to Treat Cancer. *Frontiers in Chemistry* **2020**, *8*, https://doi.org/10.3389/fchem.2020.00799.
14. Dikshit, P.K.; Kumar, J.; Das, A.K.; Sadhu, S.; Sharma, S.; Singh, S.; Gupta, P.K.; Kim, B.S. Green Synthesis of Metallic Nanoparticles: Applications and Limitations. *Catalysts* **2021**, *11*, https://doi.org/10.3390/catal11080902.
15. Qin, D.; Yang, G.; Wang, Y.; Zhou, Y.; Zhang, L. Green synthesis of biocompatible trypsinconjugated Ag nanocomposite with antibacterial activity. *Applied Surface Science* **2019**, *469*, 528–536, https://doi.org/10.1016/j.apsusc.2018.11.057.
16. Salem, S.S.; Fouda, A. Green Synthesis of Metallic Nanoparticles and Their Prospective Biotechnological Applications: An Overview. *Biological Trace Element Research* **2021**, *199*, 344–370, https://doi.org/10.1007/s12011-020-02138-3.
17. Nande, A.; Raut, A.; Michalska-Domanska, M.; Dhoble, S.J. Green Synthesis of Nanomaterials Using Plant Extract: A Review. *Current Pharmaceutical Biotechnol*ogy **2021**, *22*, 1794-1811, https://doi.org/10.2174/1389201021666201117121452.
18. Ara, M. Population Ecology and Economic Importance of *Calotropis procera* as an Exotic Medicinal Plant. *Journal of Ecology and The Natural Environment* **2017**, *1*, https://doi.org/10.23880/JENR-16000105.
19. Alghamdi, A.A.; Al-Odayni, A.-B.; Saeed, W.S.; Almutairi, M.S.; Alharthi, F.A.; Aouak, T.; Al-Kahtani, A. Adsorption of Azo Dye Methyl Orange from Aqueous Solutions Using Alkali-Activated Polypyrrole-Based Graphene Oxide. *Molecules* **2019**, *24*, https://doi.org/10.3390/molecules24203685.
20. Islam, M.R.; Rahman, M.; Farhad, S.F.U.; Podder, J. Structural, optical and photocatalysis properties of sol–gel deposited Al-doped ZnO thin films. *Surfaces and Interfaces* **2019**, *16*, 120–126, https://doi.org/10.1016/j.surfin.2019.05.007.
21. Subramanian, R.; Subbramaniyan, P.; Raj, V. Antioxidant activity of the stem bark of *Shorea roxburghii* and its silver reducing power, *SpringerPlus* **2013**, *2*, https://doi.org/10.1186/2193-1801-2-28.

22. Bansal, V.; Rautaray, D.; Ahmad, D.; Sastry, M. Biosynthesis of zirconia nanoparticles using the fungus *Fusarium oxysporum*. *Journal of Materials Chemistry* **2004**, *14*, 3303–3305, https://doi.org/10.1039/B407904C.
23. Pragya Goyal P.; Bhardwaj, A.; Kumar Mehta, B.; Mehta, D. Research article green synthesis of zirconium oxide nanoparticles (ZrO_2 NPs) using *Helianthus annuus* seed and their antimicrobial effects. *Journal of the Indian Chemical Society* **2021**, *98*, https://doi.org/10.1016/j.jics.2021.100089.
24. Davar, F.; Hassankhani, A.; Loghman-Estarki, M.R. Controllable synthesis of metastable tetragonal zirconia nanocrystals using citric acid assisted sol–gel method. *Ceramic International* **2013**, *39*, 2933–2941, https://doi.org/10.1016/j.ceramint.2012.09.067.
25. Imanova, G.T.; Agayev, T.N.; Jabarov, S.H. Investigation of structural and optical properties of zirconia dioxide nanoparticles by radiation and thermal methods. *Modern Physics Letters B* **2021**, *35*, https://doi.org/10.1142/S0217984921500500.
26. Gowri, S. Gandhi, R.R.; Senthil, S.; Sundrarajan, M. Effect of Calcination Temperature on *Nyctanthes* Plant Mediated Zirconia Nanoparticles Optical and Antibacterial Activity for Optimized Zirconia. *Journal of Bionanoscience* **2015**, *9*, 181–189, https://doi.org/10.1166/jbns.2015.1297.
27. Sathishkumar, M.; Sneha, K.; Yun, Y.-S. Green fabrication of zirconia nano-chains using novel *Curcuma longa* tuber extract. *Materials Letters* **2013**, *98*, 242-245, https://doi.org/10.1016/j.matlet.2013.02.036.
28. Majedi, A.; Abbasi, A.; Davar, F. Green synthesis of zirconia nanoparticles using the modified Pechini method and characterization of its optical and electrical properties. *Journal of Sol-Gel Science and Technology* **2016**, *77*, 542–552, https://doi.org/10.1007/s10971-015-3881-3.
29. Balaji, S.; Mandal, B.K.; Ranjan, S.; Dasgupta, N.; Chidambaram, R. Nano-zirconia –Evaluation of its antioxidant and anticancer activity. *Journal of Photochemistry and Photobiology B: Biology* **2017**, *170*, 125–133, https://doi.org/10.1016/j.jphotobiol.2017.04.004.
30. Sai Saraswathi, V.; Santhakumar, K. Photocatalytic activity against azo dye and cytotoxicity on MCF-7 cell lines of zirconium oxide nanoparticle mediated using leaves of *Lagerstroemia speciosa*. *Journal of Photochemistry and Photobiology B: Biology* **2017**, *169*, 47–55, https://doi.org/10.1016/j.jphotobiol.2017.02.023.
31. Kumaresan, M.; Anand, K.V.; Govindaraju, K.; Tamilselvan, S.; Kumar, V.G. Seaweed *Sargassum wightii* mediated preparation of zirconia (ZrO_2) nanoparticles and their antibacterial activity against gram positive and gram negative bacteria. *Microbial Pthogenes* **2018**, *124*, 311–315, https://doi.org/10.1016/j.micpath.2018.08.060.
32. Silva, F.V.; Fagundes, A.P.; Macuvele, D.L.P.; Carvalho, E.F.U.; Durazzo, M.; Padoin, N.; Soares, C.; Riella, H.G. Green synthesis of zirconia nanoparticles based on *Euclea natalensis* plant extract: Optimization of reaction conditions and evaluation of adsorptive properties. *Colloids and Surfaces A: Physicochemical Engineering Aspects* **2019**, *583*, https://doi.org/10.1016/j.colsurfa.2019.123915.
33. Parsa Rasheed, P.; Haq, S.; Waseem, M.; Ur Rehman, S.; Rehman, W.; Bibi1, N.; Ali Shah, S.A. Green synthesis of vanadium oxide-zirconium oxide nanocomposite for the degradation of methyl orange and picloram. *Materials Research Express* **2020**, *7*, https://doi.org/10.1088/2053-1591/ab6fa2.
34. Bishwokarma, M.; Bhujel, A.; Baskota, M.; Pandit, R. Green Synthesis of Zirconia (ZrO_2) Nanoparticles using *Curcuma Longa* Extract and Investigation of Compressive Strength of Epoxy resin (EP)/ZrO_2 Nanocomposites. *Journal Nepal Chemical Society* **2021**, *42*,45–50, https://doi.org/10.3126/jncs.v42i1.35328.
35. Soltys, L.; Olkhovyy, O.; Tatarchuk, T.; Naushad, M. Green Synthesis of Metal and Metal Oxide Nanoparticles: Principles of Green Chemistry and Raw Materials. *Magnetochemistry* **2021**, *7*, https://doi.org/10.3390/magnetochemistry7110145.
36. Tan, M.A.; Lagamayo, M.W.D.; Alejandro, G.J.D.; An, S.S.A. Anti-Amyloidogenic and Cyclooxygenase Inhibitory Activity of *Guettarda speciosa*. *Molecules* **2019**, *24*, https://doi.org/10.3390/molecules24224112.
37. Thu Le, H.T.; Young-Chang, C.; Cho, S. Methanol extract of *Guettarda speciosa* Linn. Inhibits the production of inflammatory mediators through the inactivation of Syk and JNK in macrophages. *International Journal of Molecular Medicine* **2018**, *41*, 1783-1791, https://doi.org/10.3892/ijmm.2018.3377.
38. Paiva-Santos, A.C.; Herdade, A.M.; Guerra, C.; Peixoto, D.; Pereira-Silva, M.; Zeinali, M.; Mascarenhas-Melo, F.; Paranhos, A.; Veiga, F. Plant-mediated green synthesis of metal-based nanoparticles for dermopharmaceutical and cosmetic applications. *International Journal of Pharmaceutics* **2021**, *597*, https://doi.org/10.1016/j.ijpharm.2021.120311.
39. Saemi, R.; Taghavi, E.; Jafarizadeh-Malmiri, H.; Anarjan, N. Fabrication of green ZnO nanoparticles using walnut leaf extract to develop an antibacterial film based on polyethylene–starch–ZnO NPs. *Green Processing and Synthsis* **2021**, *10*, 112–124, https://doi.org/10.1515/gps-2021-0011.
40. Jubu, P.R.; Yam, F.K.; Igba, V.M.; Beh, K.P. Tauc-plot scale and extrapolation effect on bandgap estimation from UV–Vis–NIR data – A case study of β-Ga_2O_3. *Journal of Solid State Chemistry* **2020**, *290*, https://doi.org/10.1016/j.jssc.2020.121576.
41. Horti, N.C.; Kamatagi, M.D.; Nataraj, S.K.; Wari, M.N.; Inamdar, S.R. Structural and optical properties of zirconium oxide (ZrO_2) nanoparticles: effect of calcination temperature. *Nano Express* **2020**, *1*, https://doi.org/10.1088/2632-959X/ab8684.

42. Gayathri, V.; Balan, R. Synthesis and Characterisation of Pure Zirconium Oxide (ZrO_2) Nanoparticle by Conventional Precipitation Method. *Journal of Environmental Nanotechnology* **2021**, *10*, 12-14, https://doi.org/10.13074/jent.2021.12.214447.
43. Reddy Yadav, L.S.; Shilpa, B.M.; Suma, B.P.; Venkatesh, R.; Nagaraju, G. Synergistic effect of photocatalytic, antibacterial and electrochemical activities on biosynthesized zirconium oxide nanoparticles. *The European Physical Journal Plus* **2021**, *136*, https://doi.org/10.1140/epjp/s13360-021-01606-6.
44. Angeline Mary, A.P.; Thaminum Ansari, A.; Subramanian, R. Sugarcane juice mediated synthesis of copper oxide nanoparticles, characterization and their antibacterial activity. *Journal of King Saud University–Science* **2019**, *31*, 1103–1114, https://doi.org/10.1016/j.jksus.2019.03.003.